PERMANENT MAGNET SOLENOID FOR A HIGH-EFFICIENCY KLYSTRON*

N. Catalan Lasheras[†,1], J. Lucas[2], I. Pompa[2], Z. Un Nisa[3], I. Syratchev[1]
[1]CERN, Geneva, Switzerland
[2]Elytt, Madrid, Spain
[3]University of Lancaster, Lancaster, UK

Abstract

Since a number of years, energy efficiency has become a priority for particle accelerators both in operation and under design. Klystrons and other RF sources have been the subject of revision in order to decrease energy consumption and increase their beam to RF efficiency. However, ancillary systems like HV systems and electromagnets can be a non-negligible power sink and may spoil the gain obtained so hard. After successfully operating a superconducting magnet as a solenoid for a high-efficiency klystron since 2022, we have designed and built a permanent magnet (PM) solenoid for a similar vacuum tube that will bring the consumption of the magnetic system to zero. We will present the design, construction and final measurements of the first prototype, but also illustrate the challenging path to this proof of principle and further optimization. From the design of the solenoid to the simulations of the electron beam inside the vacuum tube, or the necessary re-design of input and output waveguides and collector. Lessons learned are as important as the results themselves towards the transfer of this technology to any other klystron currently in the market.

INTRODUCTION

To maintain the electron beam transversely confined inside an electron vacuum tube, a static magnetic field is applied along the axis of propagation of the beam. The magnetic field is usually generated using electromagnetic coils, which represent a significant proportion of the total power consumed by the system, reducing its overall efficiency. This is especially true in pulsed systems in which RF is generated at a low duty cycle, while the magnet is powered all the time.

CERN has recently developed an 8 MW peak power high-efficiency X-band klystron in collaboration with CANON ETD that reaches 57% electron beam to RF efficiency [1]. Nevertheless, the confining solenoid consumes a total power of 9 kW, while the rest of the system working in pulsed mode is responsible for 18 kW for a final RF power of 6.4 kW. The total efficiency of the full system is thus only 23.7%. By exchanging the electromagnet for a net zero consumption PM solenoid, system efficiency is boosted to 35.5%

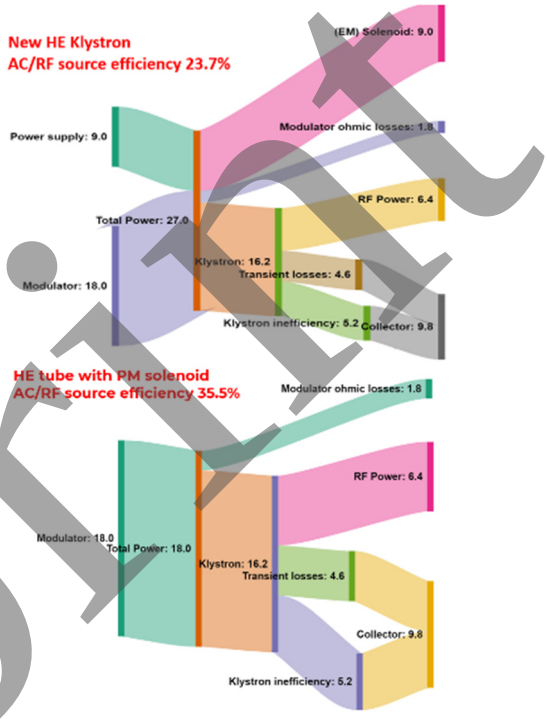

Figure 1: Contribution of each component of the RF source to the overall efficiency of the system.

In this contribution, we propose to substitute the electromagnet for an array of permanent magnets entirely removing the consumption of the magnetic system. Sankey plots shown in Fig. 1 demonstrate the impact of this change on the total efficiency of the RF system. To these benefits we should add the fact that there is no heat generation at the coil and no need for a cooling circuit further reducing the power consumption and the capital investment.

MAGNETIC DESIGN

Figure 2 shows the reference field profile as provided by the electromagnet VT-68956 delivered with the klystron E37117 manufactured by CANON ETD. It provides a maximum field about 427 mT and a non-zero field of $B_0 = 3.65$ mT at the cathode location which is key to achieve laminar flow right after the electron gun.

* Funded through the European Union's Horizon 2020 Research and Innovation programme under Grant Agreement No 101004730.
† nuria.catalan.lasheras@cern.ch

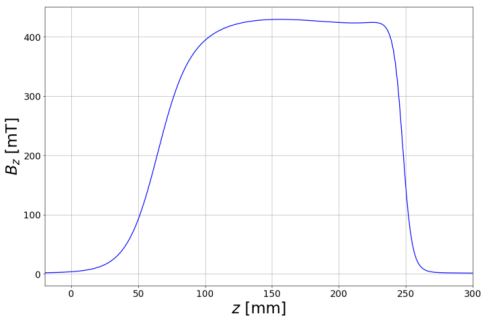

Figure 2: Longitudinal magnetic field provided by the original electromagnet.

Based on previous research [2] and past projects at ELYTT, the main building blocks chosen for the PM structure were N38[6] NdFeB blocks [3] with constant magnetization, either in the radial ($\hat{r}$) direction or in the axial ($\hat{z}$) direction in the cylindrical coordinate system. For simplicity, they are referred to as radial magnets (RM) and axial magnets (AM).

In practice, a perfectly radially magnetized cylinder is not possible to obtain with high precision. Therefore, each ring is formed by 16 PM sectors or wedges separated by a distance L=2 mm between them, as shown in Figure 3. Each trapezoidal block has a magnetization parallel to the trapezoid height.

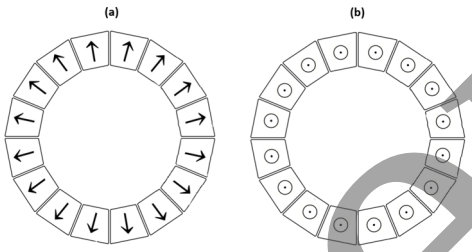

Figure 3: Arrangement of 16 radial (a) or axial (b) permanent magnets in a block.

The dimensions that characterize each PM segmented ring are the inner and outer radii $r_1$and r_2, and the axial limits z_1 and z_2. Therefore, these values were tuned for each group of PM, to get a better match with the reference magnetic field. After an iterative process, the model shown in Figure 4 was obtained, in which an entire structure of eight radial and axial blocks surrounds the tube from the electron gun to the collector region.

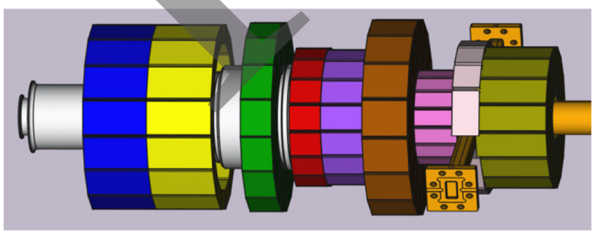

Figure 4: Final arrangement forming the solenoid built by eight blocks of symmetrically arranged PMs.

The first two blocks are located inside the oil tank of the modulator and ensure a smooth increase of the field at the level of the cathode. The middle four blocks determine the value of the field, approximately 427 mT, at the drift tube of the klystron. Lastly, the last two blocks determine the decaying of the field to zero after the output cavity.

The comparison of the magnetic field with the original electromagnet field can be seen in Figure 5. The field inversions seen before and after the required profile are a result of the zero integral property. Indeed, the field produced by a PM in the absence of a current source has a null integral. As the electron beam is generated at the cathode ($z = 0$) the field reversal at the left of that point does not affect the performance of the klystron. However, the large field reverse at the collector locations has important consequences for the beam dynamics. Indeed, at this point, we find axial electrons with no velocity that are accelerated back into the tube similarly to a magnetic bottle. A further optimization of the collector position and geometry is necessary, but it lays outside the scope of this contribution.

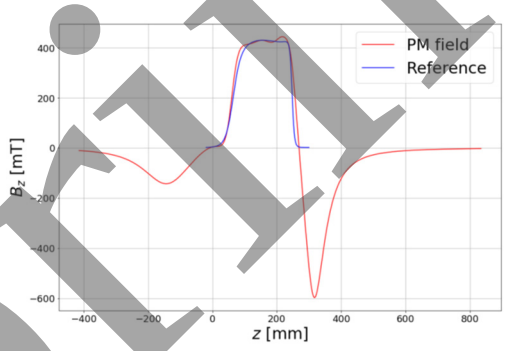

Figure 5: Longitudinal magnetic field provided by the main electromagnet and by the PM solenoid.

To achieve this field, changes are required on the klystron side for integration purposes. The magnetic material must be located as close as possible to the electron channel. For this reason and to avoid the loss of azimuthal symmetry, the output waveguide would need to be modified to exit as the same position as the input waveguide.

Simulations were done to assess the response of the electron beam to such a magnetic profile. We performed numerical simulations using DGUN [4] and CST [5]. For calibration purposes, a simulation was performed using the reference magnetic field as input. Figure 6 shows that the beam traverses the drift tube without losses. It was also observed that beam envelope modulation, also called scalloping is very low, almost achieving laminar flow.

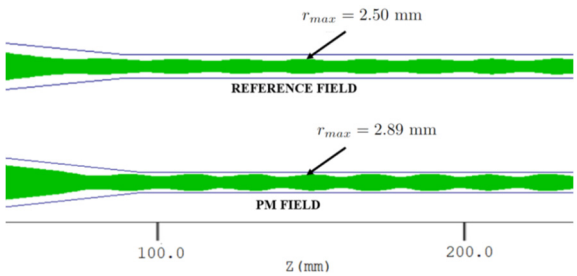

Figure 6: Beam envelope obtained by simulation using the reference field (top) or the PM field (bottom).

The reference field was then replaced with the magnetic field obtained with RADIA [6], which also gave 100%

transmission. However, compared with reference design, scalloping is more significant due to the greater variations of B_z. The beam still stays within the safety margin inside the drift tube. However higher interception losses may be expected.

Full simulations using the Particle-In-Cell (PIC) solver from CST Studio Suite were performed. These required 3D maps of the magnetic field along all the klystron volume, being highly consuming in time and computations. The results proved that undesired radial forces coming from the asymmetry of block 7, where the input and output waveguides are located, caused the electron beam to oscillate along the drift tube dangerously approaching the wall. To mitigate this, block 7 was redesigned to add a symmetry plane.

SENSITIVITY ANALYSIS

The process of manufacturing PM blocks involves several steps of machining, such as extrusion, sintering and other thermal processes [7]. Magnetizing the blocks requires strong external static fields that can present inhomogeneities [8] and magnitude variations. Additional impurities in the crystalline structure of the PM could also change the direction of the magnetization between otherwise identical blocks. For these reasons, systems made of PM are more sensitive to imperfections than those made of coils.

A sensitivity analysis was conducted in which the parameters r_1, r_2, z_1, z_2 for each PM block, each with standard uncertainties of approximately 0.1 mm, were varied simultaneously, along with the magnetization vector $\overrightarrow{M}$ in both magnitude (±1%) and direction. When errors are added, the transverse components cause deflections in the trajectory, that oscillate due to the B_z confinement field. A total of 100 simulations were performed to obtain statistical distributions, yielding a standard deviation of the axial magnetic field component B_z on the order of 1 mT. The maximum deviation, 1.32 mT, was observed at the end of the drift tube, corresponding to 0.39% of the peak magnetic field amplitude. The magnetic field at the cathode is, however, approximately 40 times more sensitive to PM block errors in relative terms. The observed deviations in B_0 can only be compensated by incorporating a correcting coil into the magnetic system, requiring a current density bellow ±0.38 A/mm².

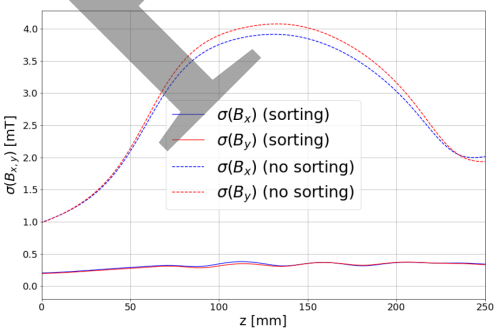

Figure 7: Standard deviations σ(B_x) and σ(B_y) at the klystron axis before and after sorting the magnets, showing a reduction by an order of magnitude.

To reduce further the impact of the statistical errors a genetic-algorithm-based sorting procedure was introduced. It assumes that the PM blocks will be measured prior to installation. The algorithm indicates the position of each of the 16 PM wedges in the ring as to minimize axial fields. Results from sorting all 100 seeds yield a reduction of the transverse magnetic field components, B_x and B_y, by up to an order of magnitude as shown in Fig. 7. The analysis demonstrates that errors in the permanent magnet (PM) blocks can be mitigated to a level at which they no longer significantly affect the electron beam within the tube.

PROTOTYPE

A physical demonstrator of the solenoid has been manufactured. It is not intended to be installed in the current klystron, but it would allow us to verify the magnetic field simulation results and field compensation techniques discussed above, including magnet measurements. Full manufacturing drawings were done as final stage of the design phase including the magnets, the mechanical support and the assembly and magnetic measurement tooling. Support and tooling represented a challenge due to the strong forces exerted by the magnets between them, reaching the order of several kN. Individual measurements on each magnet were done in order to apply sorting. The final prototype under construction can be seen in Figure 8.

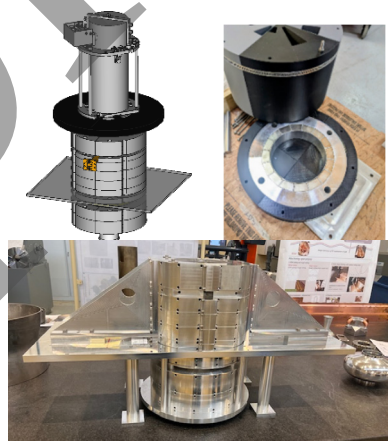

Figure 8: Assembly of the prototype. Top left: model of the total klystron/solenoid system including the oil tank interface. Top right: Assembly of one of the ring PMs. Bottom: mechanical frame made of aluminium.

CONCLUSION

A permanent magnet system capable of providing the required magnetic field strength and homogeneity for guiding the electron beam in a high-efficiency klystron has been designed and fabricated. The implementation of such a system could significantly reduce overall power consumption specially in pulsed RF sources. A prototype has been produced and experimentally tested, demonstrating the feasibility of the approach. However, further modifications of the klystron geometry would be necessary to meet the specific requirements of the permanent magnet configuration.

REFERENCES

[1] N. Catalan Lasheras *et al.*, "High-efficiency klystrons from a dream to a reality", in *Proc. IPAC'24,* Nashville, TN, May 2024, pp. 3933-3938. doi:10.18429/JACoW-IPAC2024-FRYD1

[2] Y. Fuwa and Y. Iwashita, "Performance evaluation of a klystron beam focusing system with anisotropic ferrite magnet", *Prog. Theor. Exp. Phys.*, vol. 2017, no. 2, Feb. 2017. doi:10.1093/ptep/ptw190

[3] Arnold Magnetics Technologies, Neodymium iron boron magnets, Accessed: 2024-03-25, Mar. 2024. https://www.arnoldmagnetics.com/products/neodymium-iron-boron-magnets

[4] A. Larionov and K. Ouglekov, "DGUN-code for simulation of intensive axial-symmetric electron beams," in *Proc. of 6th ICAP*, Darmstadt, Germany, 2000, p. 17.

[5] CST, https://www.3ds.com/products/simulia/cst-studio-suite

[6] RADIA, https://www.esrf.fr/home/Accelerators/instrumentation--equipment/Software/Radia.html

[7] J. Cui *et al.*, "Manufacturing Processes for Permanent Magnets: Part II—Bonding and Emerging Methods", *JOM*, vol. 74, no. 6, pp. 2492–2506, Feb. 2022. doi:10.1007/s11837-022-05188-1

[8] N. Kawasaki *et al.*, "Magnetizing technique for permanent magnets by intense static fields generated by HTS bulk magnets: Numerical Analysis", *Physics Procedia*, vol. 27, pp. 188–191, 2012. doi:10.1016/j.phpro.2012.03.442